

Sloshing and scaling: results from the Sloshe1 project

H. Bogaert^(1,2), S. Léonard⁽³⁾, L. Brosset⁽³⁾, M.L. Kaminski⁽¹⁾

¹MARIN, Hydro Structural Services, Wageningen, The Netherlands

²Delft University of Technology, Ship Structures Laboratory, Delft, The Netherlands

³GTT (Gaztransport & Technigaz), Liquid motion department, Saint-Rémy-lès-Chevreuse, France

ABSTRACT

At the turn of 2007 *full scale wave impact tests* have been carried out by MARIN in the frame of the Sloshe1 project. Unidirectional breaking waves were generated in a flume in order to impact an instrumented transverse wall with embedded test structures. The main goals of these tests were to study the hydro-elastic effects associated with the NO96 membrane containment system for LNG carriers and to create a sound database for validation of numerical simulations. The preliminary results were overviewed in 2009 by Brosset *et al.* Since then the full scale tests have been repeated at scale 1 to 6 in order to study the scaling effects. These tests are referred to as the *large scale tests*.

The large scale test set-up mimicked as far as possible the full scale set-up. At both scales the instrumentation consisted of multiple pressure sensors, accelerometers and load cells. Special attention was paid to observe the shapes of the breaking waves while impacting. This was obtained by optical sensors at full scale and high speed cameras at large scale, both synchronized with the data acquisition systems. These recordings provided insight in the sloshing physics and enabled to determine characteristic quantities like the amount of entrapped air for air pocket impacts and the corresponding oscillation frequencies.

In order to compare deterministically measured impact pressures at both scales a similarity must be ensured on the global flow from the wave paddle to the instant just before the first contact with the wall. Such a similarity has not been achieved. Reasons for that are analysed and recommendations for further tests at full scale are given.

Nevertheless a comparison is proposed restrained to global parameters describing gas pocket impacts like pressure within the gas pocket, frequency of the oscillations when compressed and damping coefficient of these oscillations. The similarity at both scales is based on the surface of the gas pocket when closing.

So-called *compressibility bias* demonstrated theoretically and illustrated numerically by Braeunig *et al.*, (2009) is confirmed experimentally. The 1D simplified model of Bagnold (1939) is presented to explain the process.

KEY WORDS: Sloshing, LNG carrier, Containment System, scaling, model test, Froude, impact pressure, flume tank, breaking wave

INTRODUCTION

Sloshing assessment of a new membrane LNG carrier is always based on sloshing model tests (see Gervaise *et al.*, 2009). Such tests are performed in GTT (Gaztransport & Technigaz) with model tanks at

scale 1:40 ($\lambda = 40$) installed on the platform of a six degree of freedom hexapod. The forced motions reproduce the calculated ship motions after Froude-scaling. This means that the linear amplitudes of the motions are scaled by $1/\lambda$ and the time is scaled by $1/\sqrt{\lambda}$. The tanks are filled with water and a mixture of gases that is chosen in order the density ratio between gas and liquid is equal to the real one on board LNG ships (around 0.004). Up to 300 pressure sensors enable to capture the sloshing pressures in the impact areas.

This approach raises the question of how to scale the measured pressures from scale $1:\lambda$ to full scale. Is Froude-scaling relevant?

It is useful to consider the flow inside a partially moving tank in two parts: the global flow and the local flow in the vicinity and during the impacts.

The global flow is rather deterministic. Repeating several times the same excitations lead to impacts at the same instants and locations even for long duration tests. When changing the scale, the global flow remains the same if Froude number and the density ratio are kept unchanged. The local flow involves several phenomena including the compression of the entrapped gas fraction (gas pocket and bubbles). The impact pressures are extremely sensitive to the impact input conditions and appear as randomly distributed even for simple harmonic one degree of freedom 2D tests. Only a statistical post-processing after long duration tests enables to get repeatable sloshing loads.

The sloshing experimental modelling with model tests is based on the reasonable assumption that, according to the Froude scalability of the global flow, tests with Froude-scaled excitations generate a statistical sample of local impact input conditions that are representative of the full scale conditions.

Now, even if the input conditions of the impacts are well scaled from the global flow, the local interactions during impacts, especially between liquid and gas, have no reason to behave according to Froude-scaling.

Braeunig *et al.*, (2009) showed that Froude-scaling of the impact pressures would be relevant only if the liquid and the gas at small scale had properties in Froude agreement with the properties of respectively the liquid and the gas at full scale (Froude-scaled equations of state). Such list of properties start with Froude-scaled speeds of sound. As such technically challenging conditions are not fulfilled yet during model tests, a compressibility bias is inevitable.

In the present study, results of wave impact tests at two different scales are presented. Two different facilities were used. The test set-ups in both facilities are presented in next section. The objective was to

compare directly the impact pressures for series of Froude-scaled wave maker steering signals. Such a deterministic comparison is relevant only if the two following requirements are fulfilled:

- At each scale, the recorded impact pressures must repeat (with a certain tolerance) when repeating the paddle steering signal.
- The global flow must be Froude-similar for scaled steering signals. This must be true up to the last stage of development of the breaking waves before impacting the wall.

A special section is dedicated to this global flow study. The two requirements turned out not to be fulfilled satisfactorily. The intended deterministic comparison between two scales was thus not possible. However, a comparison based on the size of the gas pockets for gas pocket impacts is proposed giving results in good accordance with results from a simplified model of a 1D liquid piston pushing an entrapped pocket of gas.

TESTS SET-UP AT FULL AND LARGE SCALE

The outdoor Delta flume was selected as the full scale test facility. More details about the set-up are given in Kaminski *et al.*, (2009). The Scheldt flume was selected as the large scale (1:6) facility. Both flumes operated by Deltares are ended by a piston-type second-order wave steering system. Transverse smooth test walls were placed at the other flume ends. Both walls shown in Figure 1 were designed and instrumented by MARIN. Main dimensions for both flumes are given in Table 1.

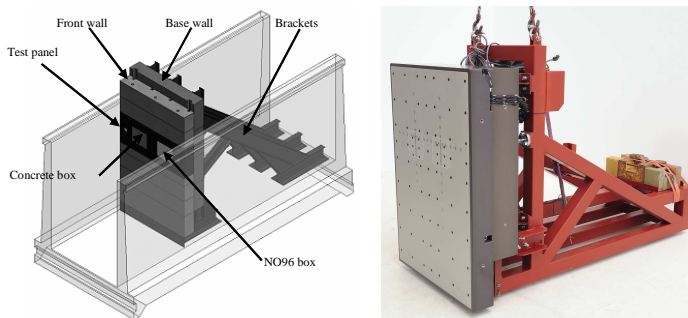


Figure 1 – Tests walls at full (left) and large (right) scales

Table 1 – Main dimensions of full and large scale facilities

	Full scale (m)	Large scale (m)
Length	240	110
Width (B)	5	1
Depth	7	1.2
Distance piston/wall (L)	143	23.63
Range of water depths (h)	3.30 – 4.25	0.625 – 0.667

The same pressure sensors were used at both scales at scaled locations with regards to the bottom and the central vertical line. The diameter of the sensitive membrane of sensors is 1.2 mm. The data acquisition system was sampling at 50 kHz during all tests.

At both scales three wave gauges were placed at a distance 4.0, 6.7, 14.7 times the water depth h from the test wall.

At full scale the shape of the waves in their last stage before breaking onto the wall was captured by the iCAM sensor consisting of a rectangular network of 640 optical sensors covering a rectangular area of 1.5 m x 3 m adjacent to the wall (see Figure 2). At large scale a high speed camera enabled to visualize the shape of the wave through the transparent wall of the flume. Its position is shown in Figure 2.

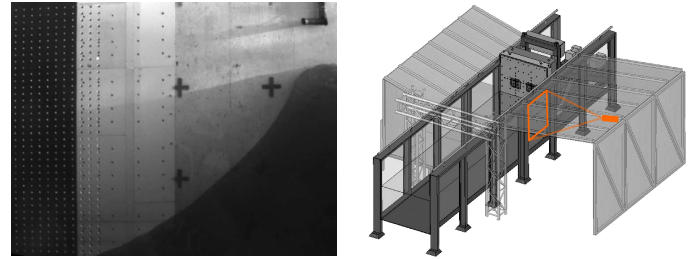


Figure 2 – iCAM sensor at full scale (left), location of the high speed camera at large scale (right)

In both facilities tests were carried out with water and air at ambient conditions. The waves were generated using a focusing method. The piston generates successive waves of increasing lengths and heights. The wave train is created in such a way that all waves add at one longitudinal position of the flume and produce a single, large breaking wave. The theoretical position where the waves meet is called the focal point.

First test campaign was dedicated to the full scale tests and was carried out in December 2006 and January 2007. The main parameters of the steering signals were tuned in order to obtain a horizontal velocity of breaking wave crest as close as possible to 10 m/s. This set of parameters is referred to as wave-type A.

Second test campaign was dedicated to the large scale tests and was carried out in April 2009. Wave-type A was first tested. However, the wave type A turned out to have two features that negatively influenced the repeatability of the flow: an unwanted leading breaking wave was always present and the wave crest was considered a not smooth enough. Therefore, a second series of tests were performed after tuning a new set of parameters referred to as wave-type B.

The main purpose of the full scale tests was to study the NO96 containment system structural behaviour under wave impacts at full scale. NO96 boxes were fixed to the wall as shown in Figure 1. New full scale tests have been just carried out in the Delta flume in April 2010, within Sloshe project, in order to study the structural behaviour of Mark III containment system. During the Mark III full scale tests, both wave types were used. An update of the scaling results will be necessary after post-processing the results with wave-type B at full scale.

GLOBAL FLOW COMPARISON AT BOTH SCALES

Ideally, one would like to compare deterministically impact pressures measured at full and large scales for different couples of Froude-scaled wave paddle signals. Such comparison makes sense only if the two conditions presented in the introduction are fulfilled: good repeatability and good similarity of the global flows until the last moment before the impact at both scales. This section checks how far these two conditions are fulfilled for the global flow.

For the repeatability at each scale, two different kinds of results are presented for series of the same paddle signal:

- Parameters of the wave elevation time trace as measured by the last wave gauge at a distance of $4.0h$ from the impacted wall. These parameters are the wave maximum height h_{max} and the last zero-crossing period T_{zc} as defined in Figure 3. Tables 2, 3 and 4 summarize the results. For each series of similar wave impacts, the mean value μ and the coefficient of variation c_v , defined as the ratio of the standard deviation to the mean, are given for both h_{max} and T_{zc} .
- The wave shape at the moment of wall impacting, as recorded by the iCAM sensor at full scale and by the high speed camera at large scale.

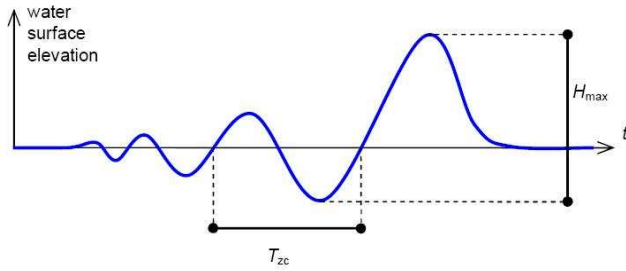


Figure 3 – Parameters of free surface elevation time trace

Repeatability at full scale (wave type A)

Only wave type A has been tested at full scale. Table 2 illustrates the repeatability of the wave elevation as measured by the last wave gauge before the wall.

Table 2 – Wave parameters h_{max} and T_{zc} as measured at 14 m of the wall for repeated paddle signals. Mean value μ and coefficient of variation c_v – Full scale – Wave type A

Impact type	Repetitions	H_{max}			T_{zc}	
		h m	μ m	c_v %	μ s	c_v %
Aerated	5	3.50	2.02	0.5	2.90	0.8
Air pocket	10	3.50	2.00	0.4	3.01	0.8
Flip-through	5	3.50	2.00	0.6	3.02	0.7
Slosh	4	3.50	1.98	1.0	3.12	0.5

At 14 m of the wall the accuracy obtained on the wave elevation for repeated paddle signals can be considered as good. For example for 10 repetitions of air pocket impacts, the coefficient of variation on the 2 m high wave after running 129 m is 0.4 (8 mm).

However, the wave shapes when impacting the wall are very different as shown in Figure 4 for three samples of these repeated air pocket impacts and in Figure 5 for three samples of repeated signals intended to induce flip-through impacts.

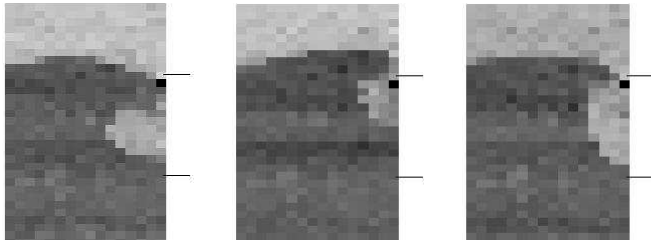


Figure 4 – Wave shapes for three air pocket impacts obtained with the same paddle signal at full scale. Time aligned with maximum pressure – Wave type A

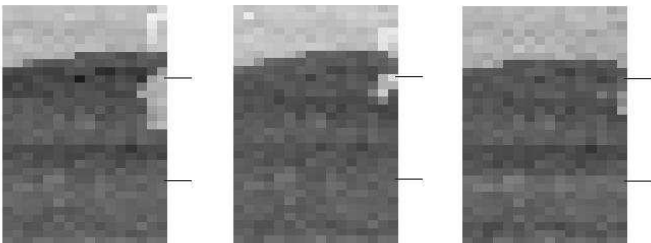


Figure 5 – Wave shapes for three flip-through impacts obtained with the same paddle signal at full scale. Time aligned with maximum pressure – Wave type A

So, the quality of the global flow repetitions clearly decreased at full scale during the last 14 meters of the wave propagation. The kind of

wave impact may even change from a flip-through to a wave packet impact as in Figure 5. The best reason to explain these discrepancies is the wind. Indeed the flume is an open air canal and even moderate varying winds as those we encountered in January 2007 north of the Netherlands, interacts strongly with the free surface while the last largest wave of the wave packet is meeting the other smaller and slower components at the focal point.

Because the global flows were clearly different for the same paddle signal, it has been concluded that the impact pressures cannot be compared deterministically.

Repeatability at large scale for wave type A

First series of tests at large scale were performed with the same type of wave paddle signal as at full scale, the wave type A. The signals were Froude-scaled. Table 3 illustrates the repeatability of the wave elevation as measured by the last wave gauge before the wall at large scale.

Table 3 – Wave parameters h_{max} and T_{zc} as measured at 2.67 m of the wall for repeated paddle signals. Mean value μ and coefficient of variation c_v – Large scale – Wave type A

Impact type	Repetitions	H_{max}			T_{zc}	
		h m	μ m	c_v %	μ s	c_v %
Aerated	5	0.667	0.395	1.0	1.25	0.2
Air pocket	3	0.667	0.377	0.2	1.32	0.2
Flip-through	5	0.667	0.373	0.3	1.35	0.3

At 2.67 m of the wall (16 m full scale) the accuracy obtained on the wave elevation for repeated paddle signals can be considered as good. For example, for 5 repetitions of flip-through impacts, the coefficient of variation on the 0.373 m high wave is 0.3 (1 mm) after running 21.17 m.

The wave shapes when impacting the wall are given respectively in Figure 6 and 7 for three repetitions of a signal inducing a wave packet impact and for three repetitions of a signal inducing a flip-through.

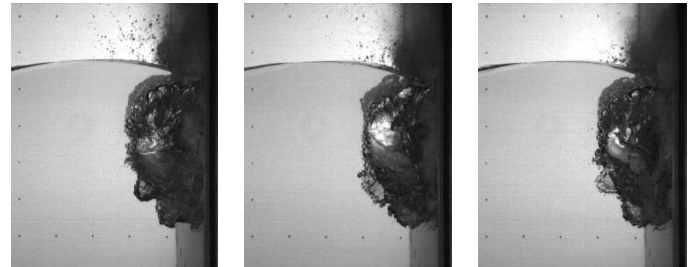


Figure 6 – Wave shapes for three air pocket impacts obtained with the same paddle signal at large scale. Time aligned with maximum pressure – Wave type A

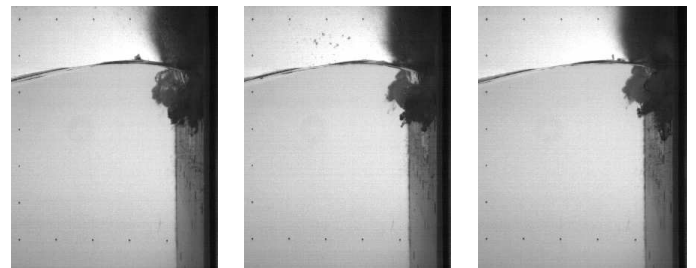


Figure 7 – Wave shapes for three flip-through impacts obtained with the same paddle signal at large scale. Time aligned with maximum pressure – Wave type A

The repeatability obtained for the global flow just before impact with wave type A at large scale is much better than at full scale. The shape of the free surface just before the impact is approximately the same for the same paddle signal. The Scheldt flume, unlike the Delta flume, was covered and no wind interfered. Nevertheless, as explained further on, the free surface looks largely disturbed and cannot be considered as deterministically determined. In these conditions there is no hope to expect repeatable impact pressures.

The main reason for these perturbations of the free surface has been found. Whatever the location of the focal point with regards to the wall, the parameters of the paddle signal as they had been tuned at first (wave type A) induced always a small leading wave (Figure 8) that brakes just in front of the focused wave.



Figure 8 – Breaking of the leading wave induced by wave type A at large scale

The remains of the broken leading wave were still present, especially at the trough level, when the main wave was approaching as can be seen on Figure 9.

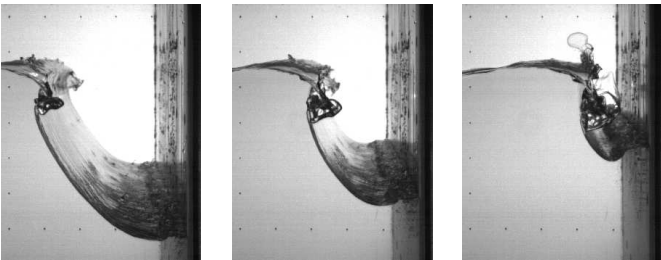


Figure 9 – Effects of the broken leading wave on the impacting wave (Wave type A – large scale)

A new set of parameters of the paddle signal has been tuned successfully in order to remove the disturbing leading wave. The new wave type is called wave type B.

Repeatability at large scale for wave type B

So, a second series of tests were performed at large scale with the wave type B. Table 4 illustrates the repeatability of the wave elevation as measured by the last wave gauge before the wall at large scale with the wave type B.

Table 4 – Wave parameters h_{max} and T_{zc} as measured at 2.5 m of the wall for repeated paddle signals. Mean value μ and coefficient of variation c_v – Large scale – Wave type B

Impact type	Repetitions	H_{max}			T_{zc}	
		h m	μ m	c_v %	μ s	c_v %
Aerated	4	0.625	0.338	0.7	1.27	0.3
Air pocket	5	0.625	0.331	0.4	1.33	0.2
Flip-through	10	0.625	0.329	0.7	1.34	0.2
Slosh	2	0.625	0.327	0.3	1.37	0.3

Here also the accuracy of the repetitions is very good at 2.5 m of the wall, at least for the free surface elevation.

The shape of the free surface when the waves impact the wall are also very repetitive as can be seen in Figure 10 for three repetitions of an air pocket impact and in Figure 11 for three repetitions of a flip-through impact. Moreover the rough appearance of the wave type A disappeared. The free surface looks much smoother since the leading breaking wave has been removed.

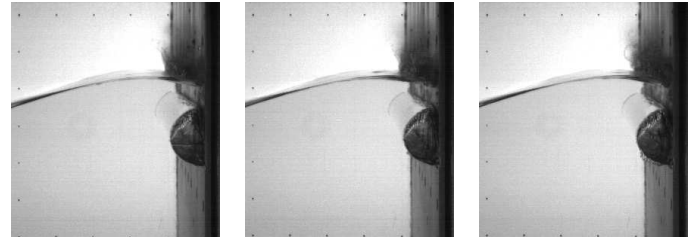


Figure 10 – Wave shapes for three air pocket impacts obtained with the same paddle signal at large scale. Time aligned with maximum pressure – Wave type B

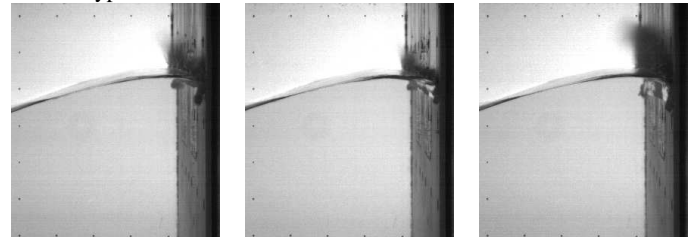


Figure 11 – Wave shapes for three flip-through impacts obtained with the same paddle signal at large scale. Time aligned with maximum pressure - Wave type B

So, as the global flow looks repeatable for the same paddle signal, it makes sense to compare more local parameters as the pressures measured by the sensors on the wall. Two different areas must be distinguished especially for air pocket impacts. All sensors inside the pocket measure the same oscillating pressure inside the pocket. At the crest level, the sensors capture the maximum pressure which occurs when the crest hit the wall. There is a sharp peak of pressure immediately followed by the slower oscillations due to the influence of the close gas pocket.

Figure 12 shows the superposition of pressure signals obtained by the same two sensors after five repetitions of the same paddle signal leading to an air pocket impact. The first sensor was located within the air pocket (left), the second sensor was located at the crest level.

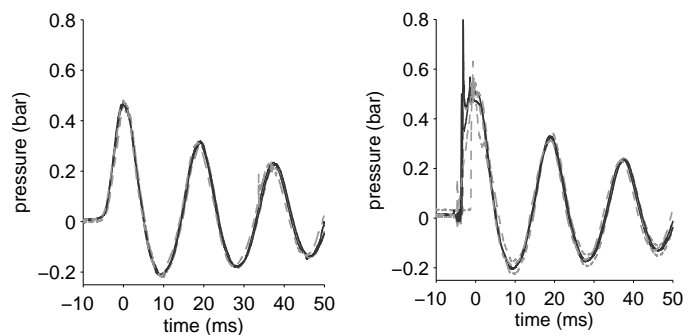


Figure 12 – Pressure in the pocket (left) and at the crest (right) for five repetitions of the same paddle signal generating an air pocket impact.

Table 5 shows the coefficient of variation c_v of the maximum pressure for the different impacts described in Table 4. Additionally, for the air pocket impact, the coefficients of variance for the air pocket pressure, frequency of oscillation and volume are given.

Table 5 – Coefficient of variation c_v of the max pressure and the gas pocket parameters for the impacts described in Table 4

	Air pocket	Flip-through c_v (%)	Slosh
Max. pressure	15	45	0.1
Air pocket pressure	2	–	–
Freq. of air pocket pres.	2	–	–
Air pocket volume	3	–	–

These results show clearly that for global air pocket parameters accurate repetitions have been achieved. When very local and sharp impact pressures are concerned as at the crest level for an air pocket impact or as during a flip-through, a good repeatability is more difficult to achieve. Still, the 15% of variation on the pressures at the crest level for five repetitions of an air pocket impact can be considered already as a good result.

Similarity of the global flows at both scales

The second requirement enabling a direct comparison of the impact pressures at both scales is to obtain accurately geometrically similar global flows for Froude-scaled paddle signals.

At both scales the paddle was a piston. So, Froude-scaling the steering paddle amplitude a_λ at scale $1:\lambda$ from the paddle amplitude a_1 at full scale, for a given focal distance x_f to the paddle, should correspond to follow the simple theoretical relation (1).

$$a_\lambda(x_f/\lambda, t/\sqrt{\lambda}) = a(x, t)/\lambda \quad (1)$$

Figure 13 compares two recorded paddle motions that should be similar at both scales.

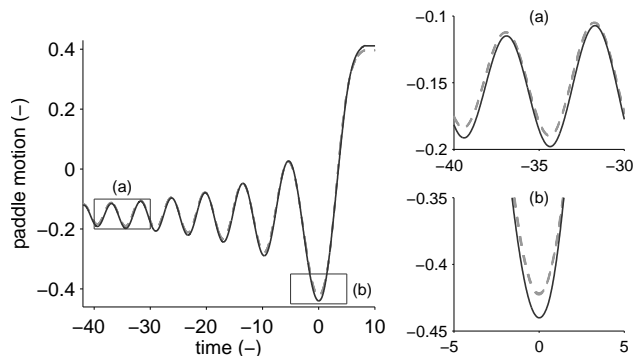


Figure 13 – Recorded paddle motions at large (-) and full (---) scales for Froude-scaled theoretical steering signals. Dimensionless translation (with h) and dimensionless time (with $\sqrt{h/g}$)

Zooms of the signals at two different stages show discrepancies that can be clearly distinguished at the trough level. In the box (a) and (b) the differences correspond respectively to about 3 cm and 8 cm full scale. This is due to mechanical difficulties for the larger piston to follow the sharp accelerations imposed by the high frequency content of the wave amplitude spectrum. Tests have shown that a transfer function can be defined to correct adequately the paddle motion.

This is more than enough to generate very different shapes of the free surface when the waves hit the wall.

COMPARISON BASED ON AIR POCKET VOLUME

From the previous section we can draw the following conclusions:

- At full scale the global flow repeats well up to around 15 m of the wall. In the last stage of the propagation the interaction between

the wind and the wave prevents a good repeatability and the shapes of the waves just before the impact may be quite different for the same paddle steering signal

- At large scale a good repeatability of the wave shape is obtained until the last stage. However the contour of the free surface is too perturbed for the wave type A. It can obviously not repeat accurately. This drawback disappears with the wave type B for which the breaking leading wave has been suppressed. Nevertheless, very local impact pressures as obtained by flip-through are still very scattered when repeating the same steering signal of the wave maker. On the other hand pressure signals measured within the gas pockets repeat accurately (around 2% on maximum pressure)
- The output paddle motions obtained from Froude-scaled theoretical steering signal do not scale very accurately. This generates waves that have not exactly similar shapes at both scales.

It is thus not possible to compare directly impact pressures obtained at both scales for Froude-scaled steering signals because the global flow is neither accurately similar nor accurately repeatable at full scale. It is still believed that a deterministic comparison at two different scales of single impacts is achievable in a flume tank. The lessons learned during this study and during another similar test campaign in the flume of Ecole Centrale Marseille (see Kimmoun *et al.*, 2010) have already been applied in the full scale tests with Mark III.

Basis for a relevant comparison at both scales

In the following, a comparison is proposed at both scales, limited to air pocket impacts that have geometrically similar areas of gas entrapped in a vertical plane, when the pocket is closing. More precisely, the reference time for the comparison of the pocket surface at both scales is the time for which the pressure at the crest level is maximal. This instant is so close to the time of first contact that it is considered that the surface of the pocket remains the same in between. At that moment the pressure inside both gas pockets is assumed as the atmospheric pressure. Figure 14 shows examples of air pockets considered as initially similar at full and large scale.

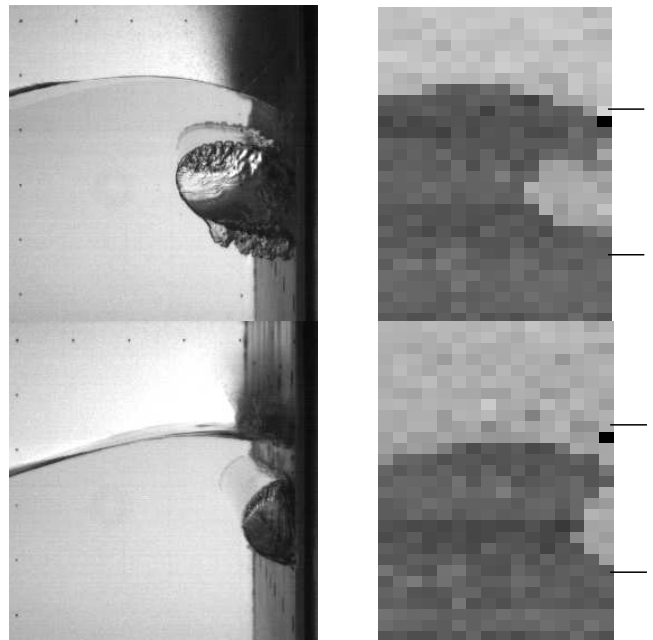


Figure 14 – Wave shapes of similar gas pockets when closing at large (left) and full (right) scales

The pocket surface is derived from such pictures as proposed in Figure 14. The accuracy is clearly better at large scale with the high speed camera pictures than at full scale with the iCAM sensor pictures.

From the instant when the pocket is closing, the global flow (considered as Froude-similar at both scales) finishes and starts the local interaction between the wave, the gas and the wall that includes the compression of the gas pocket. The study focuses now on the pocket compression at both scales.

The step by step analysis is easier at large scale. So, Figure 15 shows the shape of the free surface at large scale for a large gas pocket impact at six different instants referred to as $\tau_a, \tau_b, \tau_c, \tau_d, \tau_e, \tau_f$.

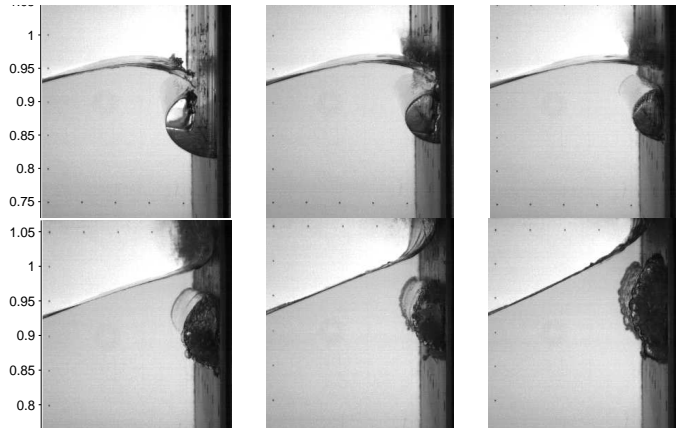


Figure 15 – Dynamic of an air pocket impact at large scale. Pressure profile and history of the gas pocket volume are given in Figure 16

The pressure time series as recorded by sensors located on the same vertical at the centre of the wall and the history of the air pocket volume (per flume width) derived manually from the high speed videos are given in Figure 16. Reference is made to the instants $\tau_a, \tau_b, \tau_c, \tau_d, \tau_e, \tau_f$ related to the pictures of Figure 15.

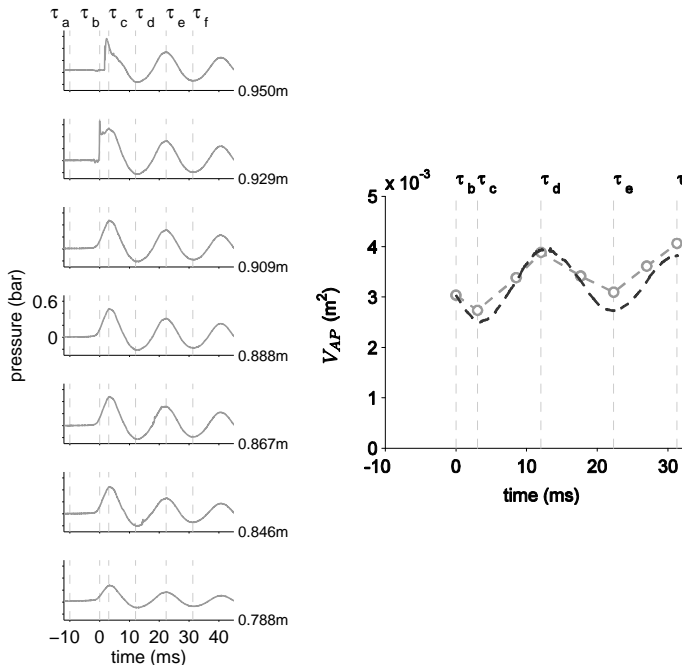


Figure 16 – Pressure profile (left) as given by sensors on the same vertical line, and time history of measured (-O-) and theoretical (- - -) air pocket volumes (right) for the impact shown in Figure 15. $\tau_a, \tau_b, \tau_c, \tau_d, \tau_e, \tau_f$ refers to the instants of the snapshots

The pressure signals given by the sensors at heights from 0.867 m to 0.909 m (at large scale) superimpose perfectly. These sensors are completely inside the air pocket. The pressure traces oscillates together with the volume of the gas pocket.

The maximum pressure is obtained at the wave crest level when the crest hits the wall at time τ_b . The maximum obtained here by the sensor at height 0.929 m is likely not the real maximum pressure on the wall as the pressure sensor density is too small to capture such localized phenomenon.

At time τ_b when the maximum pressure occurs at the crest level, the pocket is closed but the dynamic pressure (with regards to the atmospheric pressure) within the gas pocket is still zero. At time τ_c the gas pocket volume is minimal and the pressure inside is maximal. At time τ_d the volume reaches a relative maximum and the pressure is at a relative minimum. Actually from the moment the pocket is closed the relation between the volume and the pressure is governed by the equation of state of the gas. The second curve on Figure 16 (right) gives the volume history as calculated with an adiabatic equation of state derived from the pressure measurement and from the initial volume of the pocket as obtained from the picture in Figure 15 at τ_b . The assumption of the adiabatic compression is justified by the good agreement between both curves.

A general damping of the pressure oscillations is observed. An overall vertical upwards move of the pocket is also noticed, imposed by the trough run-up.

At time τ_b when the maximum pressure is reached at the crest level, the pocket has just closed and the pressure inside is still the atmospheric pressure. So, it makes sense to compare pockets that are geometrically similar at that time instance because these pockets have scaled quantities of entrapped gas. Global quantities like the gas pocket pressure, the frequency of its oscillations and the damping coefficient depend on the interaction between the flow around the pocket and the equation of state inside the pocket. For geometrically scaled initial pocket surfaces, the global flow is close to be Froude-similar but the discrepancies are not well bounded. On the other hand, the equation of state is the same at both scales and hence is not scaled properly as stated in Braeunig *et al.*, (2009). So, one would like to check as far as possible, whether this leads to a compressibility bias or not.

Comparison of the air pocket parameters at both scales

Figure 17 summarizes all results from large and full scale tests in terms of maximum pressure within the gas pocket, frequency and damping ratio of the pressure oscillations with regards to the initial pocket volume V_{AP} . Both wave types A and B were tested at large scale. Only wave type A was tested at full scale. Pressures are made dimensionless with ρgh , frequency with $\sqrt{g/h}$, volume with $h^2 B$. Froude-scaling is applicable when $p/\rho gh$ and $f/\sqrt{g/h}$ are kept the same at both scales for the same $V_{AP}/(h^2 B)$.

Considering the uncertainties of the gas pocket volume determination at full scale, the trend from the maximum pressures (Figure 17 – top – left) must be considered carefully. Nevertheless it seems that the dimensionless maximum pressures are approximately the same at both scales. It means that the gas pocket pressures scale with λ .

The trend on the frequency plot is clearer. First of all, it seems that, at large scale for a given volume V_{AP} , the frequency of the gas pocket oscillation is rather repeatable whatever the wave type is. At full scale the trend is less obvious. This has been attributed to the low accuracy of the gas pocket volume determination. Nevertheless, the dimensionless frequencies obtained at two different scales are clearly different. Actually the frequency scale here is λ instead of $\sqrt{\lambda}$ as would be expected from the Froude-scaling.

It confirms that there is a compressibility bias when performing tests at two different scales with the same gas because the gas compressibility is not scaled. This bias would increase for larger difference between the two scales.

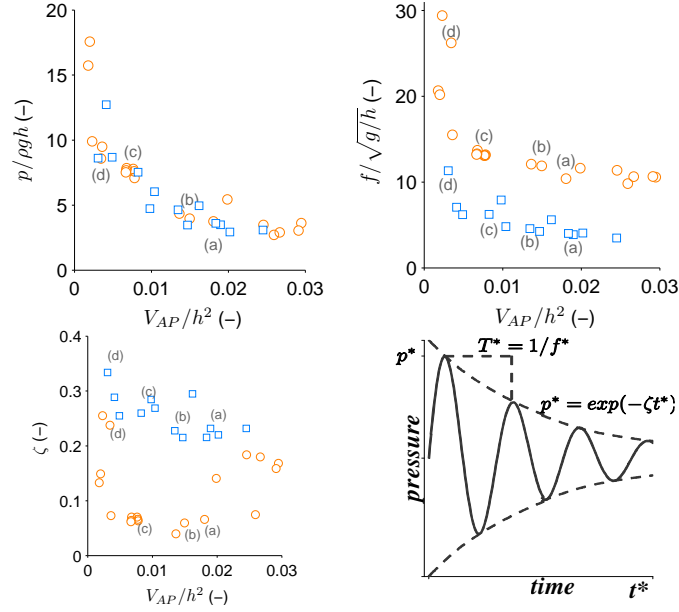


Figure 17 – Dimensionless maximum (top-left), frequency (top-right) and damping ratio ζ of pressure signals inside air pocket vs. air pocket volume for large (○) and full (□) scale tests as defined in (bottom-right).

Figure 18 illustrates further this bias by giving the superposition of pressure time histories obtained at both scales for four dimensionless initial air pocket volumes. Each case refers to a letter (a, b, c, d) which corresponds to a dot on Figure 17.

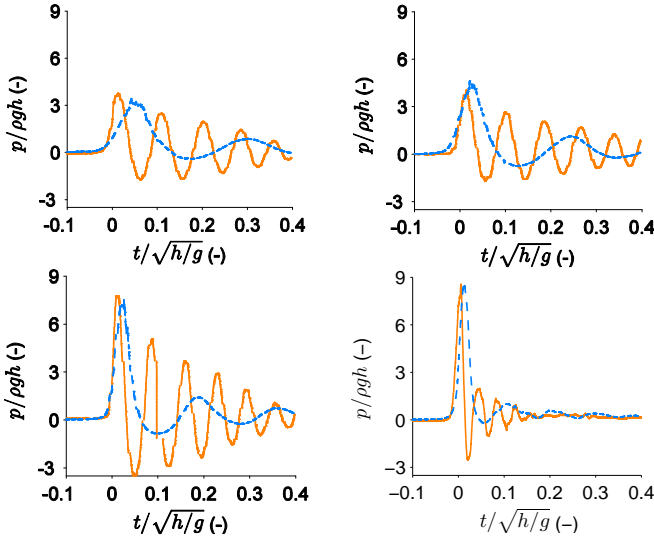


Figure 18 – Measured pressure signals inside air pockets for same dimensionless volume at large (—) and full (---) scale. $V_{AP}/h^2=0.017$ (a), 0.014 (b), 0.007 (c), 0.003 (d). These impacts refer to dots shown in Figure 17

The much higher frequency at large scale is clearly observed for every condition. Considering that the global flow is approximately Froude-scaled for geometrically scaled initial gas pocket volumes. This means

that, by reference to a simplified mass-spring system, the mass is approximately well scaled but the stiffness of the spring is not.

For geometrically scaled initial air-pocket impacts, those impacts considered at large scale lead to softer conditions after Froude-scaling than those impacts at full scale when keeping the same gas at both scales. The relatively stronger stiffness of the air pockets at large scale mitigates the impacts more than what would be expected by Froude-scaling. This induces pressure signals that are smoother at large scale than at full scale. This phenomenon would be even more pronounced for sloshing model tests at scale 1:40.

As the stiffness of the gas pocket is given by the compressibility modulus of the gas (γp_0 for a perfect gas, γ being the isentropic constant), Froude-scaling the ullage pressure at model scale by creating a partial vacuum in the tank, would scale correctly the compressibility. Unfortunately this solution cannot be envisaged for sloshing model tests as the density ratio between liquid and gas should also match at both scales (see Maillard *et al.*, 2009) and changing the ullage pressure would also directly change the density ratio. A perfect scaling is possible only with two different gases at the different scales which lead also to different liquids in order to keep the same density ratio.

During the oscillations of the pocket, the pushing mass of water is flowing around the pocket. The kinetic energy of this pushing liquid mass decreases, which could explain alone the damping observed on the pressure oscillations. Faltinsen and Timokha (2009) discussed different other damping sources including air leakage. The air leakage was further investigated by Abrahamsen and Faltinsen (2009). They concluded that these sources do not explain the observed decay: “*The system of the air pocket and the surrounding water does not obtain the same geometrical shape periodically. Hence there is no reason to expect the pressure to reproduce periodically either.*”

Following this reasoning based on the kinetic energy of the pushing water, as the oscillations are much slower in dimensionless time at full scale than at large scale, the kinetic energy lost between two oscillations is larger considering at first order a Froude-scaled flow rate of kinetic energy. This seems to be confirmed by the experimental results (see Figure 17 – bottom – left and Figure 18).

In the next section the 1D Bagnold (see Bagnold, 1939 and Mitsuyasu, 1966) piston model is studied in order to explain further the scaling issue when compressibility matters.

SIMPLIFIED BAGNOLD 1D MODEL

Comparison of Bagnold and Sloshel air-pocket impacts

A one-dimensional liquid piston is considered as described in Figure 19. The liquid of density ρ_l and length L compresses a gas pocket against a rigid wall. Initially the gas pocket has a length x_0 and a pressure p_0 . The initial velocity of the piston is U_0 . The ullage pressure on the other side of the piston keeps the constant value p_0 .

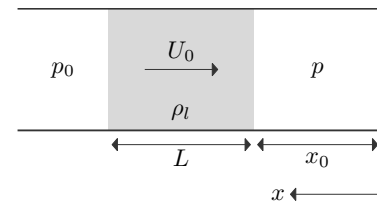


Figure 19 – Main parameters of the one-dimensional piston model of Bagnold

It is assumed the liquid is incompressible and that the gas is perfect and compressed in a quasi-equilibrium way, so that the pressure is uniform throughout the pocket. Moreover the process is considered as adiabatic.

From the continuity equation and the equation of state for perfect gas following an isentropic process, it comes immediately:

$$p = p_0 (x_0/x)^\gamma \quad (2),$$

where p is the pressure in the pocket when its length is x and γ is the isentropic constant.

The equation of motion for the piston can now be expressed as:

$$\rho_l L d^2x/dt^2 = p_0(x_0/x)^\gamma - p_0 \quad \text{with } x(0) = x_0, dx/dt(0) = -U_0 \quad (3)$$

Let us define dimensionless variables that will be indexed by *:

$$t^* = t U_0/x_0 \quad \text{and} \quad x^* = x/x_0.$$

Equation (3) becomes:

$$S (d^2x^*/dt^{*2}) = (1/x^*)^\gamma - 1 \quad \text{with } x^*(0) = 1, dx^*/dt^*(0) = -1 \quad (4)$$

and $S = (\rho_l U_0^2 L) / (p_0 x_0)$ (5) being the so-called *impact number*.

Eq. (4) is rewritten as a system of first order differential equations and integrated numerically for $\gamma = 1.4$ (air at standard conditions).

The results are summarized in Figure 20. The calculated pressure inside the air pocket is shown as a function of the impact number S , characterized by the maximum pressure p_{max} , minimum pressure p_{min} , rise time t_r and natural period $T = 1/f$.

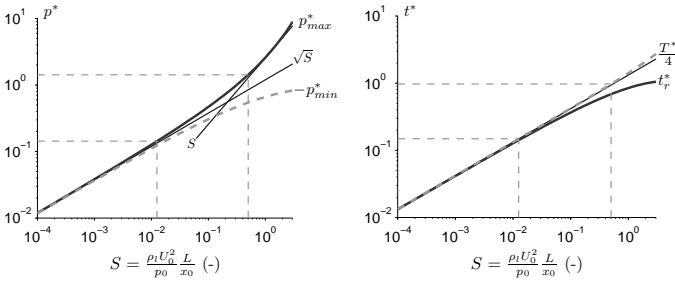


Figure 20 – dimensionless characteristics of the pressure signal in the gas pocket for Bagnold 1D model vs. the *impact number* S - Left: p_{max}^* and p_{min}^* , Right: t_r^* and T^*

Referring to the dimensionless values of the pressure $p^* = (p-p_0)/p_0$, of the rise time t_r^* and of the natural period T^* , the curves of Figure 20 show that for small values of S (at least for $S < 0.01$), thus for soft impacts, we have: $p_{max}^* \approx \sqrt{S}$ $p_{min}^* \approx -\sqrt{S}$ $t_r^* \approx T^*/4 \approx \sqrt{S}$

So, the crest and the trough of the oscillations have equal amplitude and the period is four times the rise time. This defines a sine curve.

When S keeps increasing, so, when the impacts are getting stronger, p_{max}^* deviates significantly from the \sqrt{S} line and tends towards a linear behavior with regards to S . At the same time p_{min}^* departs from the \sqrt{S} line for smaller values and the rise time becomes progressively smaller than the fourth of the period. This characterizes sharper peaks separated by larger troughs. The natural period keeps the same trend on a large range of S : $T^* \approx 4\sqrt{S}$

The maximum pressure and the period behaviors are summarized by:

$$p_{max}^* \approx S^\alpha, \quad \text{with } \alpha=0.5 \text{ for } S < 0.01 \text{ and } \alpha=1 \text{ for } S > 1 \quad (6)$$

$$T^* \approx 4\sqrt{S} \quad (7)$$

Actually a simple asymptotic development shows that for

$$S \rightarrow \infty \quad p_{max}^* \rightarrow S^\alpha \quad \text{with } \alpha = \gamma / (\gamma - 1). \quad \text{For } \gamma = 1.4 \text{ it comes } \alpha = 3.5.$$

For a full scale air-pocket impact of 50 cm diameter at full scale, Sloschel data base helps determining an order of magnitude of the impact number. Bagnold-equivalent parameters can be determined very roughly: $x_0 \approx 0.5 \text{ m}$, $U_0 \approx 5 \text{ m/s}$, $L \approx 1 \text{ m}$ leads to $S_1 \approx 0.5$. So, the variation of α in the range 0.5 to 1 seems to cover the range of S at full scale.

Figure 21 illustrates the two different behaviors of the pressure histories inside the gas pocket for impact numbers: $S_1 = 0.5$ and $S_2 = 0.0125$.

Obviously, the Bagnold model cannot describe the damping of the pressure oscillations observed during the Sloschel tests. Nevertheless the shapes of the pressure signals for soft or tough impacts as shown in Figure 21 looks very much like those obtained during the tests as shown in Figure 18 either for large or full scale. The model seems able to describe, in a simplified way, the interaction between the pushing liquid and the resisting gas that happens during a 2D gas pocket impact. The comparison is pushed further in the next sub-sections.

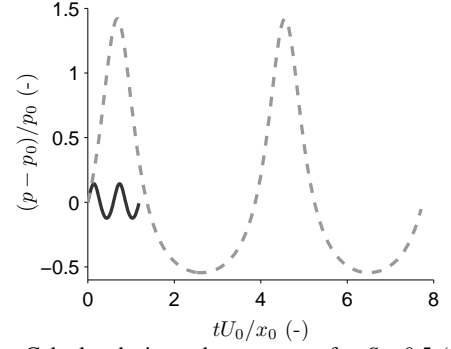


Figure 21 – Calculated air pocket pressure for $S_1=0.5$ (- -) and $S_2=0.0125$ (—).

Bagnold model and Partial Froude Scaling

In this sub-section parameters at scale 1 are indexed with 1 while parameters at scale $1/\lambda$ are indexed with λ .

According to Braeunig *et al.*, (2009), *Partial Froude Scaling* (PFS) refers to impact conditions at two different scales for which the excitations are Froude-scaled but the other phenomena involved during the sloshing impacts are not properly scaled. This wording is relevant when comparing gas-pocket impacts at full and large scales with Froude-similar global flows but with the same liquid and the same gas at both scales, as was done during the Sloschel tests.

Transposed to the Bagnold model, PFS conditions mean that the liquid and gas pocket lengths are geometrically scaled, that the liquid has an initial velocity which is Froude-scaled from full to large scale and that ρ_l and p_0 are kept the same at both scales. From the definition of the impact number given in (5), this leads to the relation $S_1 = \lambda S_2$ (8) between the two impact numbers at both scales.

The scaling law between the two impacts at different scales depends on the regions where the two values of S are located:

If both S_1 and S_2 are small (lower than 0.01), the impacts at both scales can be considered as soft impacts and relation (6) applies with $\alpha=0.5$. So, $(p_{max}^*)_1 = \sqrt{S_1}$ and $(p_{max}^*)_2 = \sqrt{S_2}$. Thus, relation (8) becomes:

$$(p_{max}^*)_1 \approx \sqrt{\lambda} (p_{max}^*)_2 \quad \text{for } S_1 < 0.01 \quad (9)$$

If both S_1 and S_2 are large (larger than 1), the impacts at both scales can be considered as hard impacts and relation (6) applies with $\alpha=1$. So, $(p_{max}^*)_1 = S_1$ and $(p_{max}^*)_2 = S_2$. Relation (8) becomes:

$$(p_{max}^*)_1 \approx \lambda (p_{max}^*)_2 \quad \text{for } S_2 > 1 \quad (10)$$

Now, in case S_1 is large (larger than 1) and S_2 is small (smaller than 0.01), relation (6) applies with $(p_{max}^*)_1 = S_1$ and $(p_{max}^*)_2 = \sqrt{S_2}$. Thus, relation (8) becomes:

$$(p_{max}^*)_1 \approx \lambda (p_{max}^*)_2^2 \quad \text{for } S_2 < 0.01 \text{ and } S_1 > 1 \quad (11)$$

So, according to Bagnold model, when the Partial-Froude-Scaled impacts are soft at both scales, the maximum dynamic pressures in the gas pockets scale with $\sqrt{\lambda}$. This is more likely to happen when both scales are small (the resistance of the air is thus favored against the kinetic energy of the liquid) and not too different (in order to remain in

the same region of S). This result is correlated by tests in the laboratory flume of Ecole Centrale Marseille (Fr) (see Kimmoun *et al*, 2010).

When the Partial-Froude-Scaled impacts are hard at both scales, the maximum pressures in the gas pockets scale with λ , This is more likely to happen when both scales are large (liquid kinetic energy is favored against resistance of air) and close (same region of S). This is confirmed by the Sloshel comparison between full and large (1:6) scales as illustrated in Figure 17 (top - left) and Figure 18.

Relations (7) and (8) lead to $T^*_I = \sqrt{\lambda} T^*_\lambda$ for a large range of S . Coming back to dimensional variables, it comes:

$$\boxed{T_I = \lambda T_\lambda \text{ and } f_I = f_\lambda / \lambda \text{ for a large range of } S} \quad (12)$$

So, according to Bagnold simplified model, the frequencies scale in $1/\lambda$ instead of $1/\sqrt{\lambda}$ as would be the case after a Froude-scaling. This result is in good agreement with Sloshel results as shown in Figure 17 (top-right).

Now, comparing global-flow-similar impacts in PFS at very different scales, as for example with sloshing model tests at scale 1:40, with the same liquid and gas at both scales, compared to full scale, leads most of the time to compare very different regions of S according to relation (8). So, most of the time, a hard impact at full scale (with $S_I=0.5$ for instance) will lead to a soft impact at small scale ($S_\lambda=0.0125$). Figure 20 illustrates the respective locations of the two impacts on the p^*_{max} -vs.- S curve and the t^* -vs.- S curve. Figure 21 illustrates these two different behaviors in terms of pressure history. A compressibility bias will spoil the results for impacts involving the compressibility of the gas. As far as the Bagnold model is relevant, the pressures within the gas pockets should scale according to (11) rather than Froude-scale.

Bagnold model and Complete Froude Scaling

According to Braeunig *et al.*, (2009), *Complete Froude Scaling* (CFS) refers to impact conditions at two different scales for which the excitations are Froude-scaled and all the other phenomena involved during the sloshing impacts are also properly scaled. This leads to keep constant the density ratio between the gas and the liquid at both scales in order to scale appropriately the incompressible gas escape phase. This leads also to scale the equation of state of the gas in order to scale appropriately the compressibility effects. Under these experimentally challenging conditions, the impact pressures Froude-scale.

Transposed to the Bagnold model, this leads to Froude-scale the ullage pressure ($p_{0I} = \lambda (p_{0\lambda})$) in order to keep constant the impact number at both scales $S_I = S_\lambda$. Thus, the balance between the pushing liquid and the resisting gas is the same at both scales, and the dimensionless pressure p^* and the dimensionless time t^* remains the same at both scales: $p^*_I = p^*_\lambda$ and $t^*_I = t^*_\lambda$ which leads to the Froude-scaling of the dimensional variables: $p_I = \lambda p_\lambda$ and $t_I = \sqrt{\lambda} t_\lambda$.

If p_0 is the atmospheric pressure at full scale, Froude-scaling the pressure at scale $1/\lambda$ is theoretically possible only with a partial vacuum at constant temperature or with reduced temperature at ambient pressure.

These solutions could be envisaged practically for the Bagnold model only because there is no escape possible for the gas. When dealing with sloshing model tests, this escaping of the gas phenomenon is important and the density ratio must be kept constant (see Maillard *et al.*, 2009). Reducing the ullage pressure or the temperature would lead to a reduction of the gas density. A parallel reduction of the liquid density would thus be required. The best practical solution for sloshing model tests would be to find a gas with as low compressibility modulus as possible (it means also an as low speed of sound as possible) in order to get closer to the ideal CFS conditions. Thus very heavy gases are necessary which imposes to adopt also heavy liquids for keeping the right density ratio.

CONCLUSIONS

How to perform wave impact tests to be compared at two different scales?

In the frame of the Sloshel project, waves breaking on a wall were generated by a focusing technique at two different scales (full scale and 1:6 referred to as large scale) in two different flume tanks equipped with paddle-type wave makers. While the geometrical ratio was kept the same for the distance between the paddle and the wall, for the water depth at rest and the focal point location, it turned out to be challenging to obtain geometrically scaled shapes of the waves just before impacting (similar global flows), only by Froude-scaling the steering signal of the wave maker.

Indeed small discrepancies were observed between the two paddle-signal outputs obtained from the Froude-scaled theoretical signals. Moreover the wave shapes in front of the wall were not accurately repeatable at full scale because of the wind influence in a long outdoor flume. The repetitions were much better at large scale but as the free surface looked slightly chaotic, the quality of the repetitions was spoiled. Changing the paddle signal spectrum in order to remove the disturbing influence of a small breaking leading wave improved much the quality of the wave shape at large scale and thus the repeatability of the global flow until the last instant before impacting.

These issues prevented from enabling a deterministic comparison between the impact pressures at two different scales as could have been initially expected. Nevertheless the authors are still convinced that such a comparison is possible and is very important to carry out. The recommendations for future tests aiming for such a comparison are as follows:

- If tests are performed in an outdoor canal, take any measure to prevent the influence of the wind. For the Mark III Sloshel full scale tests performed in April 2010, tents have been installed in order to cover the main part of the canal.
- Remove as far as possible the high frequency content from the steering signals spectrums. Indeed this high frequency content leads to very small and quick oscillations at the beginning of the imposed paddle motion. These small oscillations are difficult to follow mechanically with a good accuracy by the paddle. This was the main cause of the lack of similarity between the paddle output signals at both scales. This was also the main cause of the chaotic shape of the free surface at large scale before the correction.
- Check step by step the similarity of the global flow at both scales from the paddle signal to the shape of the free surface just before the impact. Indeed the comparison of the pressures makes sense only if the global flows are Froude-similar. At each step, if there is a discrepancy, it should be compensated by modifying the transfer function of the paddle that is applied on the theoretical wave amplitude spectrum.

These recommendations have already been applied during the Sloshel full scale tests with MarkIII containment system in April 2010.

Scaling pressures inside gas pockets

The repetitions at large scale of air-pocket impacts with the same paddle signals for the improved signal type (wave-type B) were very accurate in terms of pressure inside the pockets. As the direct comparison of impact pressures at both scales for Froude-scaled steering signals turned out not to be relevant, a comparison based only on the pressure within gas pockets for geometrically similar gas pockets at the closure time was undertaken.

Considering the small variety of wave studied, this comparison is based

on the assumption that for a given size of an air pocket at the instant when the crest is hitting the wall, the flow around the pocket is approximately the same. Until this instant, the gas behavior when the wave gets closer to the wall is incompressible. So, this instant is the end of the global flow period and the beginning of the period for local interactions between the liquid flow and the compressible gas flow.

For the scales considered (1 and $1/\lambda=1/6$) the scaling ratio for the pressures inside the gas pockets appears to be close to λ . The scaling factor for the frequencies of the oscillations appears to be also close to λ . These ratio and factor are not to be generalized! In a parallel study Kimmoun *et al.*, (2010), comparing carefully scales 1:7.5 and 1:15 in a small laboratory flume obtained a scaling ratio of $\sqrt{\lambda}$ for the pressures inside the gas pockets and the same scaling factor of λ for the frequencies.

Apparently these results are in contradiction. However, all these results are in good correlation with the results obtained from a Bagnold-type 1D simplified model of liquid piston pushing on an entrapped gas pocket. This model enables to sort the impacts according to a dimensionless parameter (impact number) which reflects the balance between the pushing liquid and the resisting gas. When the pushing liquid dominates (high impact number), the impact is hard with sharp peaks of pressure. When the cushioning effect dominates (low impact numbers), the impact is soft with pressure oscillating according to a quasi-sine curve.

When comparing Froude-similar impacts but with the same ullage pressure and the same liquid at both scales (conditions referred to as Partial Froude Conditions), the model shows that the balance between the pushing liquid and the resisting gas is necessarily biased (different impact numbers) which induces a bias of the Froude-scaling on both the pressures and the frequencies: the smaller the scale, the larger the cushioning effect. Hence, the larger the difference between the two scales, the larger the bias.

Nevertheless, when the impacts at both scales can be considered as soft, the maximum pressure scales with $\sqrt{\lambda}$. This is more likely to occur for small scales as studied by Kimmoun *et al.*, (2010). When the impacts at both scales can be considered as hard, the maximum pressure scales with λ . This is more likely to occur for large scales as in Sloschel tests.

For a large range of impact numbers, the frequencies of the oscillations scale with λ which correlates with both Kimmoun's and Sloschel results.

Consequences on the sloshing model tests

From this simple model comes another important conclusion: the only way to enable the right balance between liquid and gas actions during Froude-similar impacts at two different scales is to keep the impact factor the same. This leads to Froude-scale the ullage pressure for the simple piston model without possibility for the gas to escape.

For sloshing model tests, the gas escaping phenomenon during impacts is a major phenomenon which is ruled by the density ratio between gas and liquid. Creating a partial vacuum in the model tank in order to Froude-scale the atmospheric pressure that is considered inside LNG tanks is feasible. The initial gas would have to be very heavy in order the density ratio with regards to the water density matches the real one (around $4 \cdot 10^{-3}$) after pumping. This appears practically impossible at least at scale 1/40. The alternative is to choose an ullage gas with a scaled equation of state compared to the equation of state for Natural Gas. This leads to choose also a very heavy gas at atmospheric pressure and also a heavy liquid in order to match the density ratio. This solution appears also as not feasible.

The solution adopted by GTT consists in tests at scale 1/40 with water and a heavy gas at ambient conditions. The heavy gas is a mixture that is tuned in order to match the density ratio. The compressibility

modulus of the gas is much reduced compared to air but still too high with regards with the ideal scaled target. A compressibility bias cannot be avoided.

New full scale tests have been performed in April 2010 with the MarkIII containment system. Tests that have been performed at scale 1:6 with the improved wave type B have been mimicked at full scale following all conclusions drawn from the previous tests for enabling an optimal deterministic comparison at both scales. The conclusions presented in this paper will be updated with the new results.

ACKNOWLEDGEMENTS

The views expressed in the paper are those of the authors and do not necessarily represent the unanimous views of all the consortium members.

The authors would like to acknowledge the support provided by the Sloschel consortium members that have made the Sloschel project possible: American Bureau of Shipping, Bureau Veritas, Ecole Centrale Marseille, Chevron, ClassNK, Det Norske Veritas, Gaztransport & Technigaz, Lloyd's Register, MARIN and Shell. The support provided by the subcontractor Deltares is also much appreciated.

REFERENCES

- Abrahamsen, B., Faltinsen, O., (2009). "Decay of air cavity slamming pressure oscillations during sloshing at high fillings", Proceedings of 24th International Workshop on Water Waves and Floating Bodies, April 19-22, Zelenogorsk, Russia.
- Bagnold, R., (1939). *Interim report on wave-pressure research*, J. Inst Civil Eng. **12**: 201–226.
- Bogaert, H., Kaminski, M., (2010) "Advances in sloshing assessment from the Sloschel project", 20th (2010) Int. Offshore and Polar Eng. Conf., Beijing, China, ISOPE.
- Braeunig, J.-P., Brosset, L., Dias, F., Ghidaglia, J.-M., (2009). "Phenomenological study of liquid impacts through 2D compressible two-fluid numerical simulations", 19th (2009) Int. Offshore and Polar Eng. Conf., Osaka, Japan, ISOPE.
- Braeunig, J.-P., Brosset, L., Dias, F., Ghidaglia, J.-M., Maillard, S., (2010). "On the scaling problem for impact pressure caused by sloshing", to be submitted to a scientific journal (June, 2010?).
- Brosset, L., Mravak, Z., Kaminski, M., Collins, S., Finnigan, T., (2009) "Overview of Sloschel project", 19th (2009) Int. Offshore and Polar Eng. Conf., Osaka, Japan, ISOPE.
- Faltinsen, O., Timokha, A., (2009). "Sloshing", Cambridge University Press.
- Gervaise, E., de Sèze, P.E., Maillard, S., (2009) "Reliability-based methodology for sloshing assessment of membrane LNG vessels", 19th (2009) Int. Offshore and Polar Eng. Conf., Osaka, Japan, ISOPE.
- Kaminski, M., Bogaert, H., (2010). "Full-Scale Sloshing Impact Tests Part I", International Journal of Offshore and Polar Engineering **20**: 1–10.
- Kimmoun, O., Ratouis, A., Brosset, L., (2010) "Sloshing and scaling: experimental study in a wave canal at two different scales", 20th (2010) Int. Offshore and Polar Eng. Conf., Beijing, China, ISOPE.
- Maillard, S., Brosset, L., (2009) "Influence of density ratio between liquid and gas on sloshing model tests results", 19th (2009) Int. Offshore and Polar Eng. Conf., Osaka, Japan, ISOPE.
- Mitsuyasu, H. (1966). "Shock pressure of breaking wave", Proc. of 10th Int. Conf. Coastal Eng.

Copyright ©2010 The International Society of Offshore and Polar Engineers (ISOPE). All rights reserved.